



OPEN ACCESS

EDITED BY
Wei Zhang,
Guizhou University, China

REVIEWED BY
Sabir Hussain,
Mir Chakar Khan Rind University,
Pakistan
Ghulam Sarwar Solangi,
Sindh Agriculture University, Pakistan

*CORRESPONDENCE
Xiudao Yu,
yuxiudao@163.com

SPECIALTY SECTION
This article was submitted to
Invertebrate Physiology,
a section of the journal
Frontiers in Physiology

RECEIVED 27 July 2022
ACCEPTED 22 August 2022
PUBLISHED 13 September 2022

CITATION
Kuang Y, Xiong Y, Chen XD and Yu X
(2022), Antennae-abundant expression
of candidate cytochrome P450 genes
associated with odorant degradation in
the asian citrus psyllid, *Diaphorina citri*.
Front. Physiol. 13:1004192.
doi: 10.3389/fphys.2022.1004192

COPYRIGHT
© 2022 Kuang, Xiong, Chen and Yu. This
is an open-access article distributed
under the terms of the [Creative
Commons Attribution License \(CC BY\)](#).
The use, distribution or reproduction in
other forums is permitted, provided the
original author(s) and the copyright
owner(s) are credited and that the
original publication in this journal is
cited, in accordance with accepted
academic practice. No use, distribution
or reproduction is permitted which does
not comply with these terms.

Antennae-abundant expression of candidate cytochrome P450 genes associated with odorant degradation in the asian citrus psyllid, *Diaphorina citri*

Yinhui Kuang¹, Yu Xiong¹, Xue Dong Chen² and Xiudao Yu^{1*}

¹Ganzhou Key Laboratory of Nanling Insect Biology/Ganzhou Key Laboratory of Greenhouse Vegetables/National Navel Orange Engineering Research Center, College of Life Sciences, Gannan Normal University, Ganzhou, Jiangxi, China, ²Entomology and Nematology Department, University of Florida, Gainesville, FL, United States

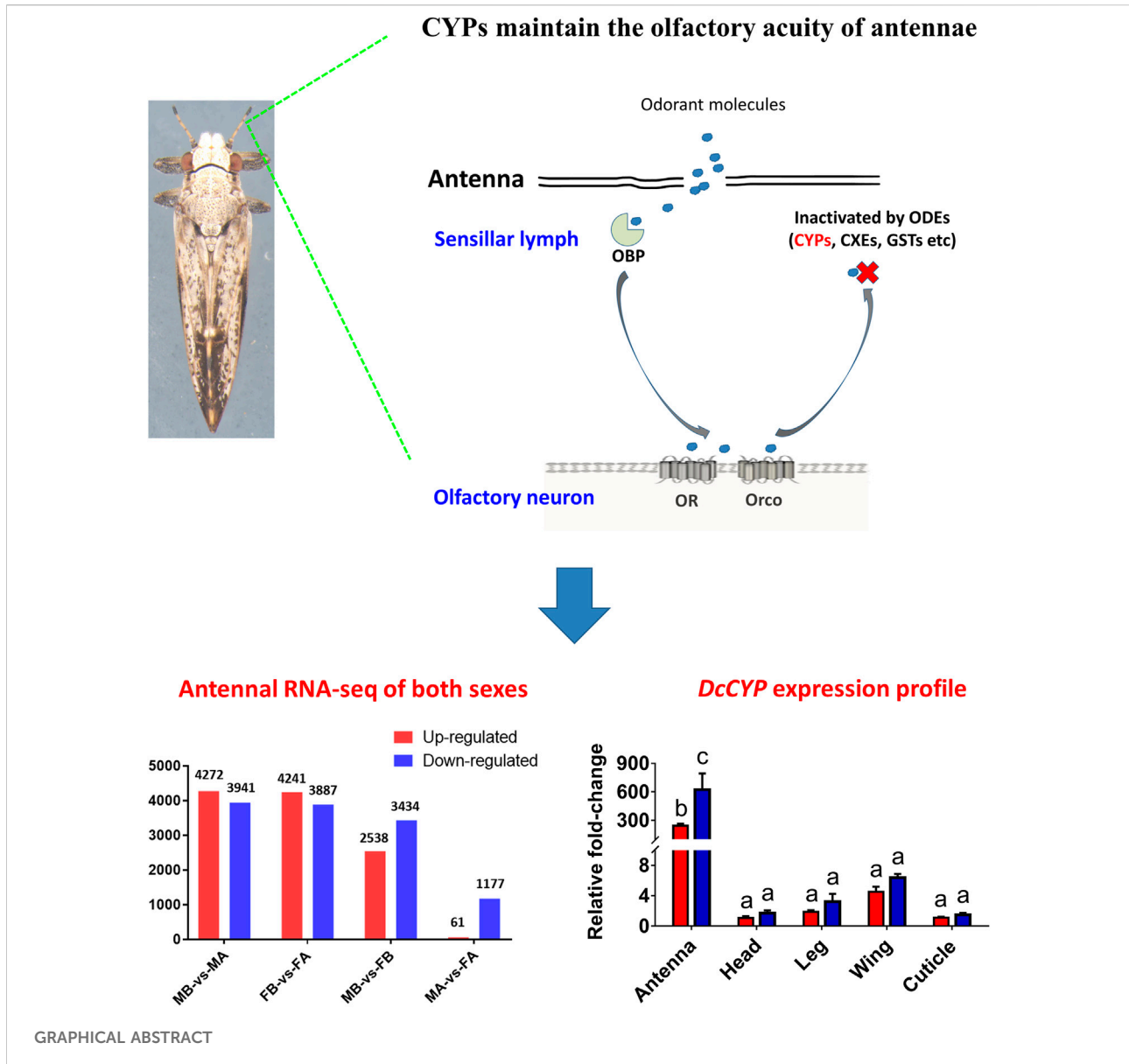
The Asian citrus psyllid, *Diaphorina citri*, is a notorious pest that is an efficient vector for *Candidatus Liberibacter asiaticus* (CLAs), the causal agent of citrus huanglongbing (HLB). The olfactory system of insects is crucial for foraging and mating behavior. Antennae-abundant odorant degrading enzymes (ODEs), including cytochrome P450 (CYPs), are important in degrading redundant odorant molecules to recover the insect olfactory. In this study, to isolate the antennal CYP genes of *D. citri*, we generated four transcriptomes from female/male antennae and body through deep sequencing of RNA libraries. Seven *DcCYP* genes preferentially expressed in antennae were first identified by comparing the antennal and body transcriptomes. Phylogenetic analysis grouped four *DcCYPs* (*DcCYP6a13*, *DcCYP6j1*, *DcCYP6k1*, and *DcCYP6a2*) into the CYP3 class, whereas *DcCYP4d2*, *DcCYP4c62*, and *DcCYP4d8* were clustered in the CYP4 clade. qRT-PCR analyses across developmental stages and tissues showed they were antennae-abundant in both genders and constantly expressed from the first instar nymph to the adult. The results presented here highlight the isolation and expression of CYP genes in *D. citri* antennae, providing valuable insights into their putative role in odorant degradation.

KEYWORDS

asian citrus psyllid, antennal transcriptome, odorant degrading enzyme, cytochrome P450, gene expression

Introduction

Insect antennae are complex sensory organs that detect various volatile compounds for securing food, mating, and oviposition. The antennal system in insects has been intensively studied using various electrophysiological, molecular, and omics techniques, providing a broad range of biological insights into olfactory perception (Oh et al., 2019; Ahn et al., 2020). The biologic processes of olfactory perception involve interactions



between exogenous odor molecules and various families of chemoreception-related proteins, including the odorant-binding proteins (OBPs), chemosensory proteins (CSPs), olfactory receptors (ORs), and odorant-degrading enzymes (ODEs) (Pelosi, 1996; Brito et al., 2016; Fleischer et al., 2018). OBPs and CSPs are small soluble proteins proposed to selectively trap and transport hydrophobic odorant molecules through the sensillum lymph towards the dendrites of olfactory sensory neurons, where ORs are located on the membrane surface (Brito et al., 2016; Cheema et al., 2021; Zhou and Jander, 2022). ORs act as a biotransducer to convert chemical signals into electrophysiological signals. Upon ORs are successfully

activated, the odor molecules must be rapidly removed by ODEs, allowing the insect olfactory system to recover and maintain the olfactory acuity (Fleischer et al., 2018; Li F et al., 2018).

ODEs play an integral role in insect chemoreception and they prevent the accumulation of stimulants and subsequent sensory adaptation (Vogt and Riddiford 1981; Younus et al., 2014). Insect ODEs have been mostly known for their involvement in the metabolism of endogenous hormones and steroids, as well as exogenous xenobiotics and allelochemicals (Younus et al., 2014; Blomquist et al., 2021). They include a few antenna-specific or antenna-enriched cytochrome P450 (CYPs), glutathione

S-transferases (GSTs), carboxylesterases (CXEs), carboxyl/cholinesterases (CCEs) and UDP-glycosyltransferases (UGTs) (Rogers et al., 1999; Maïbèche-Coisne et al., 2002; Durand et al., 2010a; Durand et al., 2010b; Keeling et al., 2013; Bozzolan et al., 2014; Tan et al., 2014; Younus et al., 2014; He et al., 2015; Li F et al., 2018; Blomquist et al., 2021; Wang et al., 2021; Wei et al., 2021). The olfactory-specific GSTs protect the olfactory system from harmful xenobiotics and inactivate the components of sex pheromone in the *Manduca sexta* and *Bombyx mori* (Rogers et al., 1999; Tan et al., 2014). In the Oriental fruit moth *Grapholita molesta*, four antenna-enriched CXEs are found to modulate foraging and mating behaviors, by hydrolyzing the acetate sex pheromone components (Z/E)-8-dodecenyl and the ester host plant volatiles (Wei et al., 2021).

CYPs represent an important supergene family of detoxification enzymes widely occurring in vertebrates and invertebrates (Nauen et al., 2022). The first antennae-specific CYP, *CYP345E2*, is functionally characterized in the pine beetle *Dendroctonus ponderosae*. This CYP enzyme catalyzes the oxidation of monoterpene pine host volatiles (Keeling et al., 2013). Subsequent studies in *D. ponderosae* document that antennae-abundant *CYP6DE1*, *CYP6DJ1*, *CYP6BW1* and *CYP6BW3*, could oxidize and remove terpenoids from antennae, as well as detoxify host terpenoids to overcome plant defenses, in which some of the terpenoid detoxification products are used as pheromones by both sexes (Chiu et al., 2019a; Chiu et al., 2019b; Chiu et al., 2019c; Blomquist et al., 2021). Examples include antennal *CYP6DE1* catalyzes the conversion of α -pinene into trans-verbenol, an aggregation pheromone released by female *D. ponderosae*; *CYP6DJ1* oxidizes terpinolene and limonene to alcohols and an epoxide, *CYP6BW1* and *CYP6BW3* oxidize several diterpene resin acids to cope with host defenses (Chiu et al., 2019a; Chiu et al., 2019b; Chiu et al., 2019c). Recent years, with antennal transcriptome analysis, some antennal CYPs have been identified in *Locusta migratoria* (Wu H et al., 2020) and *Drosophila* (Younus et al., 2014; Baldwin et al., 2021).

The Asian citrus psyllid *Diaphorina citri* Kuwayama serves as an efficient insect vector of huanglongbing (HLB) in citrus production. This disease presents an unprecedented challenge to citrus production by reducing fruit yield and quality (Yu and Killiny, 2020; Zhou, 2020). Foliar application of chemical pesticides is the major strategy for controlling *D. citri*. This is challenged by the fact that resistance development has been reported in many citrus-growing areas (Chen et al., 2018). A potential alternative and effective strategy for insect pest management *via* RNA interfere (RNAi) technique requires the selection of optimal target genes (Yu et al., 2016; Yu and Killiny, 2020). Antennae-abundant ODEs such as CYPs hold a great promise for the potential application of RNAi, in which *DcCYP*-silenced insects are expected to exhibit decreased or disordered mating and foraging behaviors.

The availability of genomic and transcriptomic data facilitated the identification of OBPs and CSPs genes in *D. citri* (Wu et al., 2016; Zhang et al., 2020; Liu et al., 2021). However, to our knowledge, no *DcCYPs* have been reported to contribute to odorant degradation. To identify *DcCYPs* correlated with odorant processing in this study, we performed as follows: 1) a comparative transcriptome analysis of antennae and body from both female and male; 2) isolation and *in silico* analysis of *DcCYPs* abundant in antennae; 3) identification of the expression profile of candidate *DcCYP* genes among tissues and developmental stages.

Materials and methods

Insect rearing

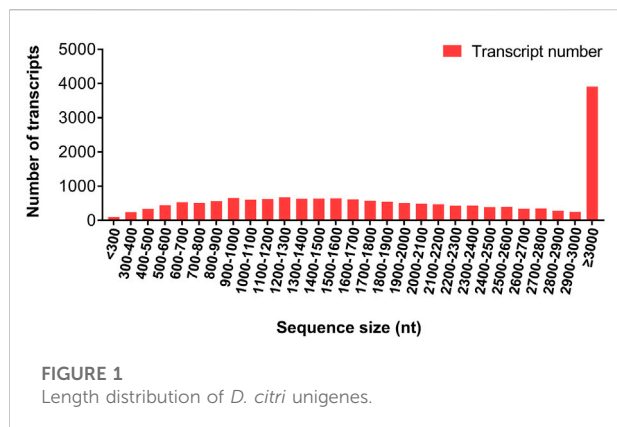
A colony of *D. citri* was collected in 2015 using field populations from Nankang District, Jiangxi (Yu et al., 2022). The culture was continuously maintained on *Murraya paniculata* seedlings in insect rearing cages kept at 27–28°C and relative humidity of 60–65% with a 14:10 h light: dark photoperiod.

Sample preparation and RNA extraction

For antennae collection, adult *D. citri* were collected using an aspirator and anesthetized with CO₂ for sex separation based on the appearance of their abdomen (Yu and Killiny, 2018). Using fine forceps, a pool of approximately 500 antennae was carefully dissected from males and females, respectively. The whole body of twenty males and females without antennae was prepared as the control. Insect samples were dissected on ice under a stereomicroscope and stored at –80°C until RNA extraction. Total RNAs were isolated from the *D. citri* tissues using Trizol (Sigma, St. Louis, MO, United States), and quantified using a NanoDrop One^c spectrophotometer (Thermo Fisher Scientific, MA, United States). The integrity of RNA was assessed on 1% agarose gels.

cDNA library construction and sequencing

cDNA library construction and Illumina sequencing of *D. citri* samples were performed at Huada Gene Sequencing Center, Wuhan, China. Briefly, Oligo (dT)-attached magnetic beads were used to purify mRNA. Purified mRNA was fragmented into small pieces to synthesize first-strand cDNA using random hexamer-primed reverse transcription, followed by second-strand cDNA synthesis. After end-repair and ligation of adaptors, the products were amplified by PCR. The double-stranded PCR products were heated, denatured and circularized by the splint oligo sequence to create a cDNA library. Pair-end sequencing of the cDNA



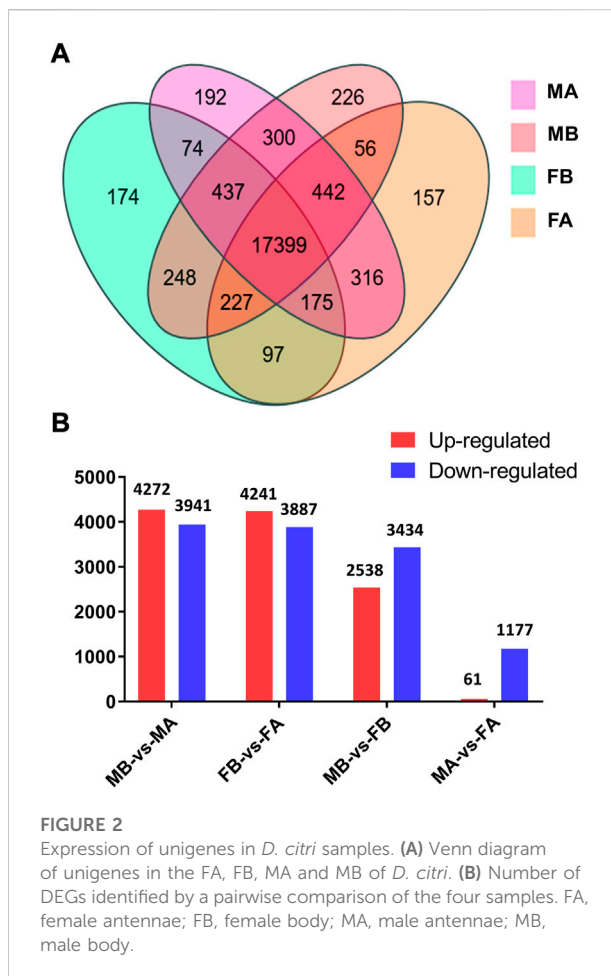
library was performed on a BGISEQ500 platform (BGI-Wuhan, China).

De novo transcriptome data processing

RNA-seq was carried out on pools of antennae and bodies from both sexes with three biological replicates. The sequencing data was filtered to obtain clean reads with SOAPnuke (v1.5.2) by removing low-quality reads (i.e., low-quality base ratio > 20%) and reads with adaptor sequences and/or unknown nucleotides (>5%). Clean reads were aligned to the reference genome [Diaci version 3.0 (Hosmani et al., 2019; Yu et al., 2022)] using HISAT2 (version 2.0.4). Transcriptome *de novo* assembly and functional annotation were conducted in BGI Company as described by Yi et al. (2021). Transcript abundances were calculated by RSEM (version 1.2.12), and differentially expressed genes among samples were determined using DESeq2 (version 1.4.5) with Q value ≤ 0.05 .

Identification and phylogenetic analysis of antennal DcCYP genes

The functional annotation of differentially expressed unigenes or contigs was performed by BLAST algorithm with a cut-off E-value of 10^{-5} in public databases, including NCBI-Nr (<http://ftp.ncbi.nlm.nih.gov/blast/db>) and Swiss-Prot (<http://ftp.ebi.ac.uk/pub/databases/swissprot>). The open reading frames (ORFs) of putative antennal DcCYP genes were predicted using the ORF finder (<http://www.ncbi.nlm.nih.gov/gorf/gorf.html>). DcCYP sequences were submitted to Pfam database (<https://pfam.xfam.org/>) and SMART (<http://smart.embl.de/>) to predict the conserved domain. The number of amino acids, molecular weights (MWs), and theoretical isoelectric points (pIs) of DcCYPs were calculated on ExPASy (<http://web.expasy.org/protparam/>). The putative N-terminal signal peptides (SPs)



of deduced DcCYP proteins were predicted using the SignalP 6.0 server (<https://services.healthtech.dtu.dk/service.php?SignalP-6.0>). The DcCYP genomic sequences were retrieved from citrusgreening.org. The exon-intron structure was determined on the Gene Structure Display Server (GSDS, <http://gsds.cbi.pku.edu.cn/>) by comparing the full-length ORF sequence with the corresponding genomic DNA sequence. The antennal DcCYPs and CYPs of *Acyrtosiphon pisum* were used for the phylogenetic analysis (Ramsey et al., 2010; Supplementary Table S1). The alignment of CYP protein sequences was performed using CLUSTAL_X (version 1.83). The joint unrooted phylogenetic tree was constructed with MEGA11 using the maximum likelihood method with 1,000 bootstrap replicates (Tamura et al., 2021).

Quantitative real-time PCR analysis

To examine the expression of DcCYP genes, a variety of *D. citri* tissues (antenna, head, leg, wing and cuticle) and samples of

TABLE 1 Twenty differentially expressed genes (DEGs) that are most abundant in *D. citri* antennae.

| Gene ID | Transcriptomic data (mean FPKM) | | | | Gene name |
|-----------------|---------------------------------|-----------------|----------------|-----------------|--|
| | FA | MA | FB | MB | |
| Dcitr09g01010.1 | 156,432 ± 11,677 | 150,360 ± 8,884 | 55,317 ± 2,664 | 53,182 ± 6,217 | uncharacterized protein LOC113469368 |
| Dcitr02g18990.1 | 16,673 ± 1,247 | 13,986 ± 1,103 | 5,375 ± 924.1 | 6,792 ± 891.4 | chemosensory protein 4 |
| Dcitr01g13620.1 | 8,716 ± 2,283 | 8,272 ± 1,622 | 13.24 ± 1.546 | 14.22 ± 0.6486 | odorant-binding protein A10 |
| Dcitr01g12900.1 | 8,008 ± 1,652 | 7,984 ± 389.5 | 13.94 ± 0.955 | 12.67 ± 0.2466 | glutathione S-transferase 1 |
| Dcitr01g03170.1 | 5,667 ± 1,264 | 5,408 ± 1,185 | 45.43 ± 4.513 | 4.223 ± 0.6045 | odorant-binding protein 6 |
| Dcitr06g09930.1 | 5,259 ± 2,255 | 4,894 ± 1,085 | 4.897 ± 1.362 | 6.623 ± 1.925 | protein yellow-like |
| Dcitr01g03210.1 | 4,862 ± 959.1 | 4,769 ± 925.6 | 69.54 ± 9.749 | 28.81 ± 3.399 | odorant binding protein 1 |
| Dcitr13g01140.1 | 3,803 ± 533.2 | 3,213 ± 399.1 | 1,250 ± 57.65 | 1,289 ± 133.1 | no hits |
| Dcitr04g02650.1 | 3,262 ± 1755 | 3,806 ± 1939 | 291.7 ± 333.5 | 495.7 ± 768.9 | cuticle protein 65 |
| Dcitr12g10130.1 | 2,911 ± 1,097 | 2,122 ± 221.7 | 685.4 ± 80.94 | 735.7 ± 88.64 | titin-like |
| Dcitr01g15840.1 | 2,830 ± 306.4 | 2,251 ± 233.7 | 1,103 ± 445.5 | 972.8 ± 117.4 | uncharacterized protein LOC103520889 |
| Dcitr08g07580.1 | 2,546 ± 727.9 | 2,555 ± 368.3 | 20.38 ± 3.375 | 0.2867 ± 0.0472 | odorant-binding protein 83a |
| Dcitr03g06540.1 | 2,186 ± 674.4 | 2,751 ± 1,084 | 654.6 ± 179.3 | 650 ± 337.7 | no hits |
| Dcitr03g01230.1 | 1806 ± 986.7 | 1,537 ± 348.2 | 0.96 ± 0.5467 | 0.74 ± 0 | no hits |
| Dcitr08g08410.1 | 1721 ± 536.5 | 1,560 ± 63.85 | 67.66 ± 21.68 | 73.71 ± 3.957 | endocuticle structural glycoprotein SgAbd-2 |
| Dcitr06g07220.1 | 1,640 ± 92.48 | 1,637 ± 76.14 | 427.6 ± 26.3 | 451.5 ± 16.93 | protein takeout-like |
| Dcitr06g09860.1 | 1,483 ± 643 | 1,362 ± 373.4 | 1.113 ± 0.9026 | 1.007 ± 0.1747 | chemosensory protein 10 |
| Dcitr09g09530.1 | 1,362 ± 150.7 | 1,315 ± 250.6 | 630.8 ± 45.92 | 832.4 ± 58.85 | uncharacterized protein LOC103517165 |
| Dcitr06g09550.1 | 1,320 ± 9.613 | 1,209 ± 135.3 | 673.4 ± 86.43 | 654.1 ± 11.78 | intracellular protein transport protein USO1 |
| Dcitr09g09520.1 | 1,237 ± 184.2 | 1,168 ± 32.43 | 89.18 ± 5.605 | 86.89 ± 4.627 | circadian clock-controlled protein |

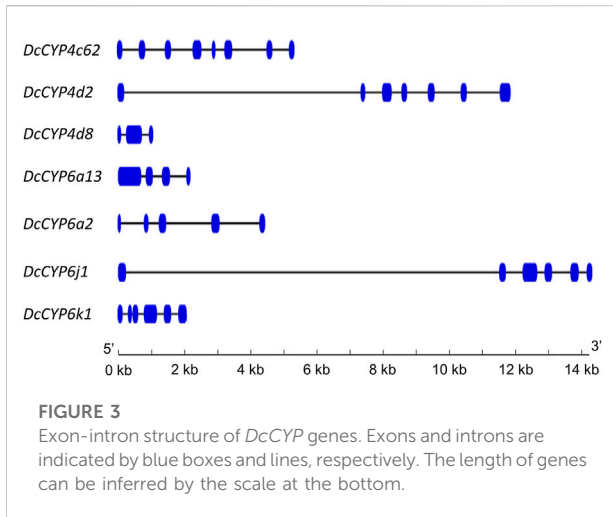
TABLE 2 Identification of candidate *DcCYP* genes in different expression values (FPKM) in the *D. citri* antennal and body transcriptomes.

| Designation | Gene ID | Transcriptomic data (mean FPKM) | | | | ORF (aa) | Mw (kDa) | pI |
|-------------|-----------------|---------------------------------|----------------|--------------|--------------|----------|----------|------|
| | | FA | MA | FB | MB | | | |
| DcCYP4c2 | Dcitr05g07670.1 | 60.71 ± 10.57 | 56.31 ± 11.59 | 8.79 ± 1.15 | 8.62 ± 1.51 | 509 | 58.56 | 6.62 |
| DcCYP4d2 | Dcitr01g21810.1 | 132.80 ± 21.67 | 167.70 ± 18.98 | 12.78 ± 0.74 | 17.07 ± 1.62 | 513 | 58.77 | 8.43 |
| DcCYP4d8 | Dcitr13g02280.1 | 21.53 ± 10.21 | 15.86 ± 3.69 | 1.60 ± 0.39 | 1.90 ± 1.28 | 249 | 28.45 | 6.14 |
| DcCYP6a13 | Dcitr02g16350.1 | 117.60 ± 43.98 | 103.30 ± 10.93 | 10.45 ± 0.14 | 14.39 ± 0.28 | 436 | 50.44 | 8.45 |
| DcCYP6a2 | Dcitr11g07150.1 | 157.70 ± 43.81 | 140.20 ± 6.02 | 17.40 ± 2.59 | 18.53 ± 3.07 | 298 | 34.29 | 8.15 |
| DcCYP6j1 | Dcitr06g01770.1 | 94.21 ± 5.01 | 94.85 ± 13.64 | 1.10 ± 0.21 | 1.38 ± 0.05 | 514 | 60.30 | 8.01 |
| DcCYP6k1 | Dcitr03g06130.1 | 58.92 ± 7.98 | 49.23 ± 4.27 | 14.41 ± 2.47 | 15.61 ± 2.60 | 449 | 52.20 | 9.04 |

aa, amino acids; Mw, molecular weight; pI, isoelectric points.

D. citri at six stages, including the first instar nymph, second instar nymph, third instar nymph, fourth instar nymph, fifth instar nymph, as well as adult male and female were collected separately. First-strand cDNA synthesis was initiated with 500–1,000 ng of purified RNA using the EasyScript® One-Step gDNA Removal and cDNA Synthesis SuperMix (TransGen Biotech, Beijing, China). The synthesized cDNA was stored at –20 C until use.

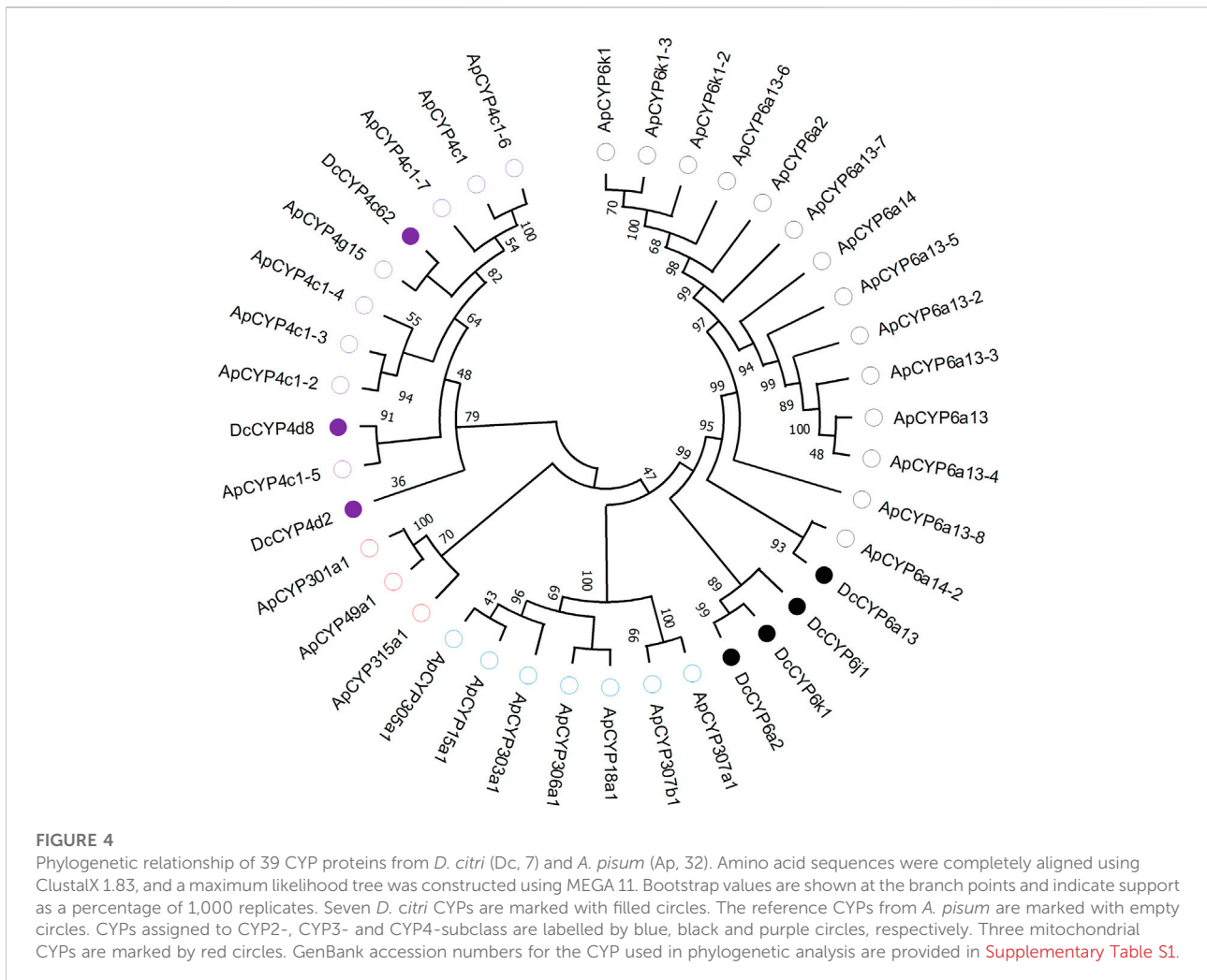
qRT-PCR reactions were carried out in a 20 µl volume: 4 µl of diluted cDNA, 0.4 µM of each primer and 10 µl of PerfectStart® Green qPCR SuperMix (TransGen Biotech, Beijing, China). All the samples were placed in a Roche LightCycler 96® system (Roche Diagnostics, Mannheim, Germany). Two reference genes, actin (GenBank accession number DQ675553) and GAPDH (GenBank accession number XM_017447140), were used to normalize the



amount of cDNA added to the PCR reactions. The relative value of *DcCYP* gene expression was analyzed using the $2^{-\Delta\Delta Ct}$ method (Livak and Schmittgen, 2001). Specific primers for each gene were listed in **Supplementary Table S2**. Three replicates were performed for each treatment.

Statistical analysis

To compare the expression level of *DcCYP* gene among different tissues and developmental stages, the ANOVA with Tukey's multiple comparisons test was performed using GRAPHPAD PRISM version 6.0 (GraphPad Software Inc., La Jolla, CA, United States). A value of $p < 0.05$ was considered statistically significant.



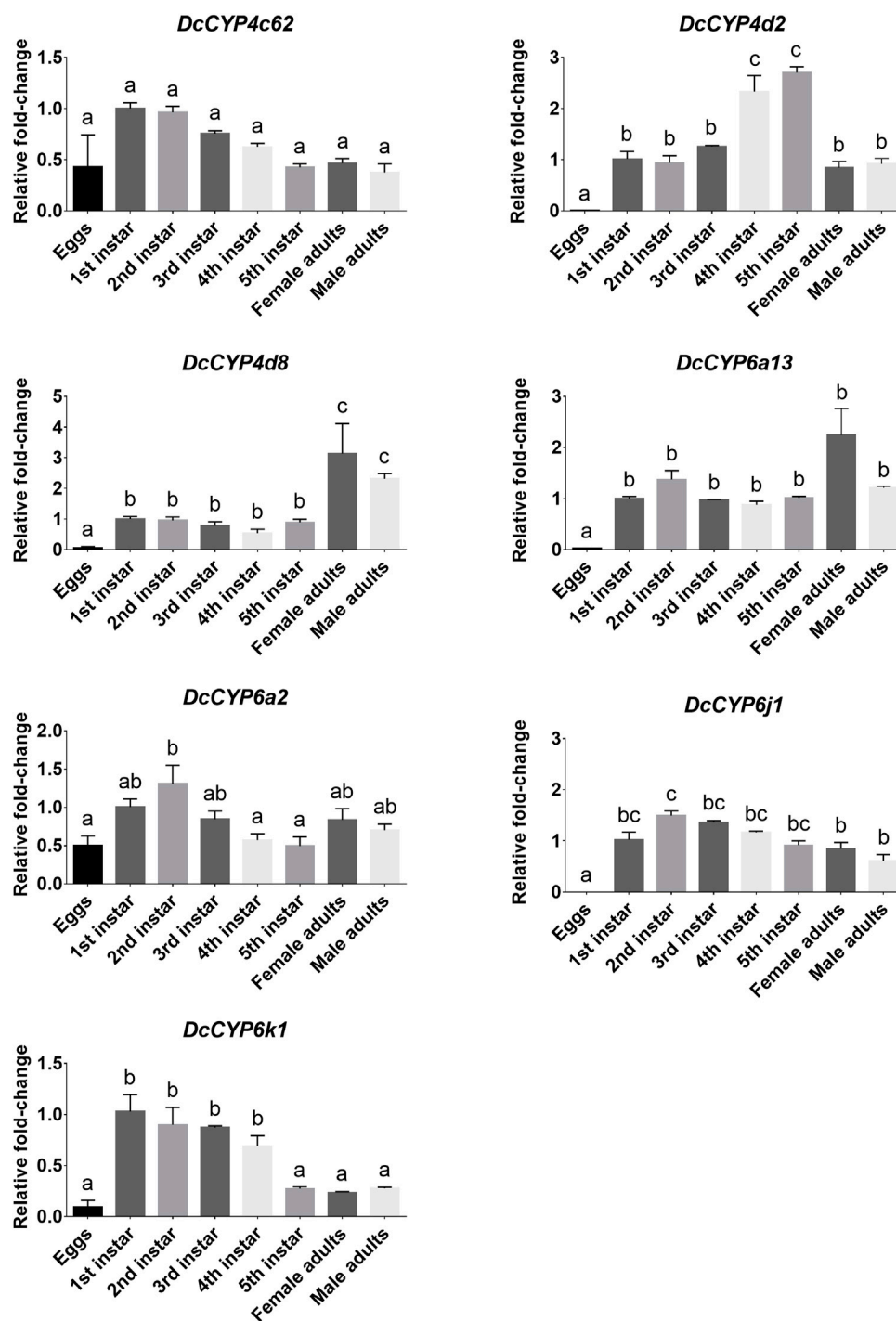


FIGURE 5
DcCYP expression at different life stages of *D. citri*. The expression level of *DcCYP* in first instar nymph was assigned an arbitrary value of 1. The expression levels in other samples are presented relative to the average first instar levels. Error bars represent standard error. Different letters above the error bar indicate significant differences among developmental stages ($p < 0.05$; one-way ANOVA, Tukey's multiple comparisons test).

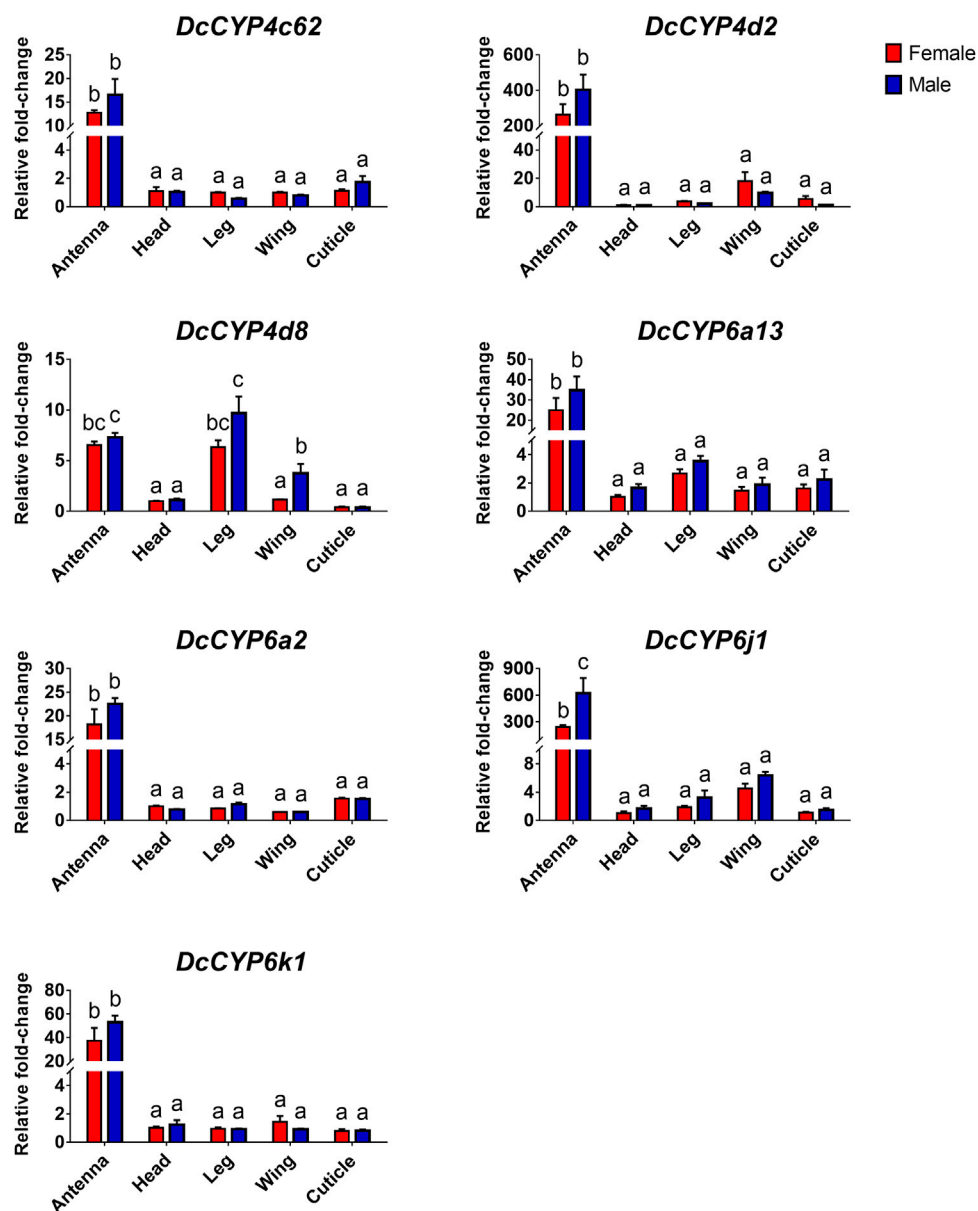


FIGURE 6
The relative abundance of *DcCYP* transcripts between different sexes and tissues. The expression level of *DcCYP* in female head was assigned an arbitrary value of 1. The expression levels in other samples are presented relative to the average female head levels. Different letters above the error bar indicate significant differences among female and male tissues ($p < 0.05$; two-way ANOVA, Tukey's multiple comparisons test).

Results

Transcriptome sequencing and analysis

Twelve RNA samples from female antennae (FA), female body (FB), male antennae (MA), and male body (MB) were sequenced using a DNBSEQ platform, with total raw reads of

45.44 M per sample. After data filtering, a total base of 6.46 ± 0.02 Gb per FA, 6.47 ± 0.03 Gb per FB, 6.45 ± 0.02 Gb per MA, and 6.48 ± 0.02 Gb per MB were generated, respectively (Supplementary Table S3). The clean data were subjected to *de novo* transcriptome assembly using Trinity software. A total of 20,520 unigenes were generated, which refer to a uniquely assembled transcript or a cluster of genes that perform a

particular function. Among them, 13,827 unigenes (67.38%) were longer than 1,000 bp, and 7,747 (37.75%) were longer than 2000 bp (Figure 1). Additionally, 17,212 (83.88%) unigenes were annotated in at least one public database (e.g. GO, KEGG, KOG, NR, NT, Pfam, and SwissProt databases), while 3,308 (16.12%) unigenes had no matching sequences in any of these databases. All RNA-seq data generated for this study were deposited in the GenBank under Bio-Project accession number PRJNA857870.

Analysis of differentially expressed genes

Comparative analyses of the antennal and body transcriptomes from both sexes in this study provide useful information to identify the antennae-specific and sex-biased antennal genes. A total of 665 unigenes were detected only in the antenna of females or males; 192 unigenes were unique for MA and 157 were expressed only in FA (Figure 2A). DEGs with a Q value ≤ 0.05 were further identified in antennae, by comparing with the transcriptomes of body tissues. Pairwise comparisons of transcript abundance revealed that 4,241 and 4,272 unigenes were significantly upregulated in FA and MA, respectively (Figure 2B). Twenty DEGs that were most abundant in antennae were listed in Table 1. These included transcripts of odorant binding protein (*DcOBP1*, *DcOBP6*, *DcOBPA10*, and *DcOBP83a*), chemosensory protein (*DcCSP4* and *DcCSP10*), etc. Notably, *DcOBP1*, *DcOBP6*, *DcOBPA10*, *DcOBP83a*, and *DcCSP10* exhibited an antennae-specific expression pattern, in which their antennal FPKM values were >100-fold higher than in the body (Table 1).

Identification of candidate *DcCYP* genes

Seven DEGs abundant in antennae were identified to be *DcCYPs* by blasting against the Nr database. Their redundancy levels were found to be 15.86–167.70 FPKM in antennae, which were >3-fold higher compared to body group. The predicted Mw was from 28.45 to 60.30 kDa with the predicted pI of 6.14–9.04. All *DcCYP* proteins harbored a conserved P450 domain (Pfam ID: PF00067), and were predicted to have no signal peptide, indicating their functional location inside the cell (Table 2). Gene structure analysis showed that the length of genomic sequence (1,116–14,366 nt) and the number of introns (2–7) varied dramatically among *DcCYP* genes (Figure 3). A maximum likelihood phylogenetic tree was constructed using the amino-acid sequence of the P450 domain from candidate *DcCYPs* and *A. pisum*

CYPs. Four subclasses (*CYP2*, *CYP3*, *CYP4*, and mitochondrial *CYP*) were well clustered in relevant phylogenetic branches. *DcCYP6a13*, *DcCYP6j1*, *DcCYP6k1*, and *DcCYP6a2* were categorized in the *CYP3* clan; the other three *DcCYP* genes, *DcCYP4d2*, *DcCYP4c62* and *DcCYP4d8* were clustered in the *CYP4* class (Figure 4).

Developmental and tissue expression analysis for *DcCYP* genes

To identify the *DcCYPs* that correlated with odorant degradation in the antennae, *DcCYP* transcripts abundant in the antennae basing on the FPKM methods were selected for developmental and tissue expression analysis. The selected *DcCYP* genes were constantly expressed from the first instar nymph to the adult, along with the low or undetectable levels detected in eggs. However, *DcCYP4d2* transcripts accumulated at a higher level in the last nymphal instar (fourth–fifth), and *DcCYP4k1* exhibited relatively higher expression in the first–fourth nymphal instar (Figure 5). Tissue expression analysis revealed that *DcCYP4c62*, *DcCYP4d2*, *DcCYP6a13*, *DcCYP6a2*, *DcCYP6j1* and *DcCYP6k1* were expressed higher in both male and female antennae than in other non-olfactory tissues, such as heads, legs, wings, and cuticles; *DcCYP4d8* had higher expression levels in the antennae and legs of both sexes (Figure 6). Interestingly, the expression of *DcCYP6j1* calculated by qRT-PCR were a bit higher in the male antennae than in the female antennae, which was inconsistent with the RNA-Seq data (Table 2; Figure 6); this possibly attributed to the difference in sensitivity of two methods.

Discussion

Chemical control of *D. citri* is threatened by the increased insecticide resistance (Chen et al., 2018). Insect antennae are the main structures responsible for odorant reception *via* sensilla (Ahn et al., 2020; Zhou and Jander, 2022). Identification of antennal ODE such as *CYP* genes, could provide insights into the odorant recognition mechanism of *D. citri* and further help us to better control this agricultural pest insect. In this study, a total of seven antennae-enriched *DcCYP* genes were first identified by comparing the antennal and body transcriptome data from both sexes. qRT-PCR analyses showed they were antenna-biased and constantly expressed from the first instar nymph to the adult, with *DcCYP6j1* expressed in male antennae at relatively higher levels.

Transcriptome analyses in this study identified several antennae-specific and/or antennae-enriched genes in *D. citri*. As expected, chemosensory gene *OBPs* and *CSPs* were highly expressed in antennae. Among the top twenty DEGs that were abundant in antennae, four transcripts were identified as *OBP* genes (*DcOBP1*, *DcOBP6*, *DcOBPA10* and *DcOBP83a*), and two DEGs were *CSP* genes (*DcCSP4* and *DcCSP10*), this was consistent with the putative olfactory role of insect antennae. Antennal *OBP* and *CSP* genes have been reported in many other insect species including spotted-wing *drosophila suzukii* (Ahn et al., 2020), ladybird *Aphidius gifuensis* (Kang et al., 2021), as well as hemipteran aphid (Zhou et al., 2010; Wang et al., 2019), hawthorn lace bug *Corythucha ciliata* (Li G. W et al., 2018) and brown plant hopper *Nilaparvata lugens* (Zhou et al., 2014). In green peach aphid *Myzus persicae*, three *OBP* genes (*MpOBP6/7/10*) were specifically expressed in antennae, and five *OBP* genes (*MpOBP2/4/5/8/9*) were expressed antennae enriched (Wang et al., 2019).

Insect CYPs perform a variety of important physiological functions, and evidence for their metabolic clearance of plant volatiles or host phytochemical detoxification is accumulating (Blomquist et al., 2021; Vandenhole et al., 2021; Nauen et al., 2022). Insect CYPs could be categorized into CYP2, CYP3, CYP4 and mitochondrial CYP clans (Feyereisen, 2012). Many members of CYP3 and CYP4 clan are currently known or suspected to participate in herbivore adaptation to host plant (Feyereisen, 2012; Blomquist et al., 2021; Vandenhole et al., 2021). For example, the CYP3 P450 genes in *Dendroctonus armandi* and *Oedaleus asiaticus* were shown to be induced by the host terpenoids (pinene and 3-carene) or flavonoid rutin (Dai et al., 2016; Huang et al., 2017); in another study, larval exposure to the plant volatiles induced by *Spodoptera litura* herbivory enhanced transcript levels of CYP3 genes (Sun et al., 2021). From the four clades of P450s commonly found in insects, we found four transcripts (*DcCYP6a13*, *DcCYP6j1*, *DcCYP6k1* and *DcCYP6a2*) were clustered in CYP3 family, and three genes (*DcCYP4d2*, *DcCYP4c62* and *DcCYP4d8*) were grouped in CYP4 clan.

Antennae-abundant CYPs have been functionally demonstrated as ODEs involved in terpenoid detoxification and odorant processing (Keeling et al., 2013; Chiu et al., 2019a; Chiu et al., 2019b; Chiu et al., 2019c; Blomquist et al., 2021). A combined transcriptome and qRT-PCR analysis in this study revealed that seven *DcCYP* genes (*DcCYP4d2*, *DcCYP4c62*, *DcCYP4d8*, *DcCYP6a13*, *DcCYP6j1*, *DcCYP6k1* and *DcCYP6a2*) were preferentially expressed in antennae. Unexpectedly, six totally different *DcCYP* genes (*CYP3175B1*, *CYP3178A1*, *CYP3640A2*, *CYP4C67*, *CYP380C15* and *CYP3167A7*) were reported to be

antennae-abundant in the previous study (Wu Z et al., 2020), by comparing antennal transcriptome with that of gut tissues, reproductive organs, Malpighia tubules, brain, and fat body. However, the selected small tissues and organs are not representatives of non-olfactory tissues, this may contribute to the conflicting results of previous studies. In addition, the expression of *DcCYP6j1* was observed to be a bit higher in male antennae. Our results, together with previous findings that male-biased CYPs were usually implicated in the recognition processes of sex pheromone (Maibèche-Coisne et al., 2004; Feng et al., 2017), suggesting a putative role of these *DcCYPs* in inactivation of plant volatile semiochemicals and/or sex pheromone. Future research elucidating their physiological role will help understand the olfactory mechanism of hemipteran insect, and offer new targets for developing behavioral interference control strategy against *D. citri*.

Data availability statement

The datasets presented in this study can be found in online repositories. The names of the repository/repositories and accession number(s) can be found below: <https://www.ncbi.nlm.nih.gov/>, PRJNA857870.

Author contributions

XY conceived the study; YK and YX reared the insects and conducted the laboratory work; XY and YK carried out the analyses; XC helped to modify the manuscript; XY wrote the manuscript.

Funding

This work is funded by the National Natural Science Foundation of China (grant no. 32160634), the Natural Science Foundation for Distinguished Young Scholars of Jiangxi province (grant no. 20212ACB215001), the Double Thousand Plan of Jiangxi Province (grant no. jxsq2019101058), and the Major Science and Technology R&D Program of Jiangxi Province (grant no. 20194ABC28007).

Acknowledgments

The authors wish to acknowledge the assistance of Yan Liu, Zhidan Hu and Fang Liang with the psyllid samples.

Conflict of interest

The authors declare that the research was conducted in the absence of any commercial or financial relationships that could be construed as a potential conflict of interest.

Publisher's note

All claims expressed in this article are solely those of the authors and do not necessarily represent those of their affiliated

organizations, or those of the publisher, the editors and the reviewers. Any product that may be evaluated in this article, or claim that may be made by its manufacturer, is not guaranteed or endorsed by the publisher.

Supplementary material

The Supplementary Material for this article can be found online at: <https://www.frontiersin.org/articles/10.3389/fphys.2022.1004192/full#supplementary-material>

References

- Ahn, S. J., Oh, H. W., Corcoran, J., Kim, J. A., Park, K. C., Park, C. G., et al. (2020). Sex-biased gene expression in antennae of *Drosophila suzukii*. *Arch. Insect Biochem. Physiol.* 104, e21660. doi:10.1002/arch.21660
- Baldwin, S. R., Mohapatra, P., Nagalla, M., Sindvani, R., Amaya, D., Dickson, H. A., et al. (2021). Identification and characterization of CYPs induced in the *Drosophila* antenna by exposure to a plant odorant. *Sci. Rep.* 11, 20530–20614. doi:10.1038/s41598-021-99910-9
- Blomquist, G. J., Tittiger, C., MacLean, M., and Keeling, C. I. (2021). Cytochromes P450: terpene detoxification and pheromone production in bark beetles. *Curr. Opin. Insect Sci.* 43, 97–102. doi:10.1016/j.cois.2020.11.010
- Bozzolan, F., Siaussat, D., Maria, A., Durand, N., Pottier, M. A., Chertemps, T., et al. (2014). Antennal uridine diphosphate (UDP)-glycosyltransferases in a pest insect: diversity and putative function in odorant and xenobiotics clearance. *Insect Mol. Biol.* 23, 539–549. doi:10.1111/imb.12100
- Brito, N. F., Moreira, M. F., and Melo, A. C. (2016). A look inside odorant-binding proteins in insect chemoreception. *J. Insect Physiol.* 95, 51–65. doi:10.1016/j.jinsphys.2016.09.008
- Cheema, J. A., Carraher, C., Plank, N. O., Travas-Sejdic, J., and Kralicek, A. (2021). Insect odorant receptor-based biosensors: Current status and prospects. *Biotechnol. Adv.* 53, 107840. doi:10.1016/j.biotechadv.2021.107840
- Chen, X. D., Gill, T. A., Ashfaq, M., Pelz-Stelinski, K. S., and Stelinski, L. L. (2018). Resistance to commonly used insecticides in asian citrus psyllid: stability and relationship to gene expression. *J. Appl. Entomol.* 142, 967–977. doi:10.1111/jen.12561
- Chiu, C. C., Keeling, C. I., and Bohlmann, J. (2019a). Cytochromes P450 preferentially expressed in antennae of the mountain pine beetle. *J. Chem. Ecol.* 45, 178–186. doi:10.1007/s10886-018-0999-0
- Chiu, C. C., Keeling, C. I., and Bohlmann, J. (2019b). The cytochrome P450 CYP6DE1 catalyzes the conversion of α -pinene into the mountain pine beetle aggregation pheromone trans-verbenol. *Sci. Rep.* 9, 1477–1510. doi:10.1038/s41598-018-38047-8
- Chiu, C. C., Keeling, C. I., Henderson, H. M., and Bohlmann, J. (2019c). Functions of mountain pine beetle cytochromes P450 CYP6DJ1, CYP6BW1 and CYP6BW3 in the oxidation of pine monoterpenes and diterpene resin acids. *PLoS One* 14, e0216753. doi:10.1371/journal.pone.0216753
- Dai, L., Ma, M., Gao, G., and Chen, H. (2016). *Dendroctonus armandi* (Curculionidae: Scolytinae) cytochrome P450s display tissue specificity and responses to host terpenoids. *Comp. Biochem. Physiol. B Biochem. Mol. Biol.* 201, 1–11. doi:10.1016/j.cbpb.2016.06.006
- Durand, N., Carot-Sans, G., Chertemps, T., Bozzolan, F., Party, V., Renou, M., et al. (2010a). Characterization of an antennal carboxylesterase from the pest moth *Spodoptera littoralis* degrading a host plant odorant. *PLoS One* 5, e15026. doi:10.1371/journal.pone.0015026
- Durand, N., Carot-Sans, G., Chertemps, T., Montagné, N., Jacquín-Joly, E., Debernard, S., et al. (2010b). A diversity of putative carboxylesterases are expressed in the antennae of the noctuid moth *Spodoptera littoralis*. *Insect Mol. Biol.* 19, 87–97. doi:10.1111/j.1365-2583.2009.00939.x
- Feng, B., Zheng, K., Li, C., Guo, Q., and Du, Y. (2017). A cytochrome P450 gene plays a role in the recognition of sex pheromones in the tobacco cutworm, *Spodoptera litura*. *Insect Mol. Biol.* 26, 369–382. doi:10.1111/imb.12307
- Feyereisen, R. (2012). "Insect CYP genes and P450 enzymes," in *Insect molecular biology and biochemistry*. Editor L. I. Gilbert (Amsterdam: Elsevier BV), 236–316.
- Fleischer, J., Pregitzer, P., Breer, H., and Krieger, J. (2018). Access to the odor world: olfactory receptors and their role for signal transduction in insects. *Cell. Mol. Life Sci.* 75, 485–508. doi:10.1007/s00018-017-2627-5
- He, P., Zhang, Y. N., Yang, K., Li, Z. Q., and Dong, S. L. (2015). An antenna-biased carboxylesterase is specifically active to plant volatiles in *Spodoptera exigua*. *Pestic. Biochem. Physiol.* 123, 93–100. doi:10.1016/j.pestbp.2015.03.009
- Hosmani, P. S., Flores-Gonzalez, M., Shippy, T., Vosburg, C., Massimino, C., Tank, W., et al. (2019). Chromosomal length reference assembly for *Diaphorina citri* using single-molecule sequencing and Hi-C proximity ligation with manually curated genes in developmental, structural and immune pathways. bioRxiv [Preprint]. doi:10.1101/869685
- Huang, X., Whitman, D. W., Ma, J., McNeill, M. R., and Zhang, Z. (2017). Diet alters performance and transcription patterns in *Oedaleus asiaticus* (Orthoptera: Acrididae) grasshoppers. *PLoS One* 12, e0186397. doi:10.1371/journal.pone.0186397
- Kang, Z. W., Liu, F. H., Xu, Y. Y., Cheng, J. H., Lin, X. L., Jing, X. F., et al. (2021). Identification of candidate odorant-degrading enzyme genes in the antennal transcriptome of *Aphidius gifuensis*. *Entomol. Res.* 51, 36–54. doi:10.1111/1748-5967.12489
- Keeling, C. I., Henderson, H., Li, M., Dullat, H. K., Ohnishi, T., and Bohlmann, J. (2013). CYP345E2, an antenna-specific cytochrome P450 from the mountain pine beetle, *Dendroctonus ponderosae* Hopkins, catalyzes the oxidation of pine host monoterpene volatiles. *Insect Biochem. Mol. Biol.* 43, 1142–1151. doi:10.1016/j.imb.2013.10.001
- Li, F., Fu, N., Li, D., Chang, H., Qu, C., Wang, R., et al. (2018). Identification of an alarm pheromone-binding chemosensory protein from the invasive sycamore lace bug *Corythucha ciliata* (Say). *Front. Physiol.* 9, 354. doi:10.3389/fphys.2018.00354
- Li, G. W., Chen, X. L., Xu, X. L., and Wu, J. X. (2018). Degradation of sex pheromone and plant volatile components by an antennal glutathione S-transferase in the oriental fruit moth, *Grapholita molesta* Busck (Lepidoptera: Tortricidae). *Arch. Insect Biochem. Physiol.* 99, e21512. doi:10.1002/arch.21512
- Liu, X. Q., Jiang, H. B., Fan, J. Y., Liu, T. Y., Meng, L. W., Liu, Y., et al. (2021). An odorant-binding protein of Asian citrus psyllid, *Diaphorina citri*, participates in the response of host plant volatiles. *Pest Manag. Sci.* 77, 3068–3079. doi:10.1002/ps.6352
- Livak, K. J., and Schmittgen, T. D. (2001). Analysis of relative gene expression data using real-time quantitative PCR and the $2^{-\Delta\Delta Ct}$ method. *Methods* 25, 402–408. doi:10.1006/meth.2001.1262
- Maibèche-Coisne, M., Jacquín-Joly, E., François, M. C., and Nagnan-Le Meillour, P. (2002). cDNA cloning of biotransformation enzymes belonging to the cytochrome P450 family in the antennae of the noctuid moth *Mamestra brassicae*. *Insect Mol. Biol.* 11, 273–281. doi:10.1046/j.1365-2583.2002.00335.x
- Maibèche-Coisne, M., Nikonov, A. A., Ishida, Y., Jacquín-Joly, E., and Leal, W. S. (2004). Pheromone anosmia in a scarab beetle induced by *in vivo* inhibition of a pheromone-degrading enzyme. *Proc. Natl. Acad. Sci. U. S. A.* 101, 11459–11464. doi:10.1073/pnas.0403537101
- Nauen, R., Bass, C., Feyereisen, R., and Vontas, J. (2022). The role of cytochrome P450s in insect toxicology and resistance. *Annu. Rev. Entomol.* 67, 105–124. doi:10.1146/annurev-ento-070621-061328
- Oh, H. W., Jeong, S. A., Kim, J., and Park, K. C. (2019). Morphological and functional heterogeneity in olfactory perception between antennae and maxillary

- palps in the pumpkin fruit fly, *Bactrocera depressa*. *Arch. Insect Biochem. Physiol.* 101, e21560. doi:10.1002/arch.21560
- Pelosi, P. (1996). Perireceptor events in olfaction. *J. Neurobiol.* 30, 3–19. doi:10.1002/(SICI)1097-4695(199605)30:1<3::AID-NEU2>3.0.CO;2-A
- Ramsey, J. S., Rider, D. S., Walsh, T. K., De Vos, M., Gordon, K., Ponnala, L., et al. (2010). Comparative analysis of detoxification enzymes in *Acyrtosiphon pisum* and *Myzus persicae*. *Insect Mol. Biol.* 19, 155–164. doi:10.1111/j.1365-2583.2009.00973.x
- Rogers, M. E., Jani, M. K., and Vogt, R. G. (1999). An olfactory-specific glutathione-S-transferase in the sphinx moth *Manduca sexta*. *J. Exp. Biol.* 202, 1625–1637. doi:10.1242/jeb.202.12.1625
- Sun, Z., Lin, Y., Wang, R., Li, Q., Shi, Q., Baerson, S. R., et al. (2021). Olfactory perception of herbivore-induced plant volatiles elicits counter-defences in larvae of the tobacco cutworm. *Funct. Ecol.* 35, 384–397. doi:10.1111/1365-2435.13716
- Tamura, K., Stecher, G., and Kumar, S. (2021). MEGA11: molecular evolutionary genetics analysis version 11. *Mol. Biol. Evol.* 38, 3022–3027. doi:10.1093/molbev/msab120
- Tan, X., Hu, X. M., Zhong, X. W., Chen, Q. M., Xia, Q. Y., and Zhao, P. (2014). Antenna-specific glutathione S-transferase in male silkworm *Bombyx mori*. *Int. J. Mol. Sci.* 15, 7429–7443. doi:10.3390/ijms15057429
- Vandenhoe, M., Dermauw, W., and Van Leeuwen, T. (2021). Short term transcriptional responses of P450s to phytochemicals in insects and mites. *Curr. Opin. Insect Sci.* 43, 117–127. doi:10.1016/j.cois.2020.12.002
- Vogt, R. G., and Riddiford, L. M. (1981). Pheromone binding and inactivation by moth antennae. *Nature* 293, 161–163. doi:10.1038/293161a0
- Wang, Q., Zhou, J. J., Liu, J. T., Huang, G. Z., Xu, W. Y., Zhang, Q., et al. (2019). Integrative transcriptomic and genomic analysis of odorant binding proteins and chemosensory proteins in aphids. *Insect Mol. Biol.* 28, 1–22. doi:10.1111/imb.12513
- Wang, M. M., Long, G. J., Guo, H., Liu, X. Z., Wang, H., Dewar, Y., et al. (2021). Two carboxylesterase genes in *Plutella xylostella* associated with sex pheromones and plant volatiles degradation. *Pest Manag. Sci.* 77, 2737–2746. doi:10.1002/ps.6302
- Wei, H., Tan, S., Li, Z., Li, J., Moural, T. W., Zhu, F., et al. (2021). Odorant degrading carboxylesterases modulate foraging and mating behaviors of *Grapholita molesta*. *Chemosphere* 270, 128647. doi:10.1016/j.chemosphere.2020.128647
- Wu, Z. Z., Zhang, H., Bin, S. Y., Chen, L., Han, Q. X., and Lin, J. T. (2016). Antennal and abdominal transcriptomes reveal chemosensory genes in the Asian citrus psyllid, *Diaphorina citri*. *PLoS One* 11, e0159372. doi:10.1371/journal.pone.0159372
- Wu, H., Liu, Y., Shi, X., Zhang, X., Ye, C., Zhu, K. Y., et al. (2020). Transcriptome analysis of antennal cytochrome P450s and their transcriptional responses to plant and locust volatiles in *Locusta migratoria*. *Int. J. Biol. Macromol.* 149, 741–753. doi:10.1016/j.ijbiomac.2020.01.309
- Wu, Z., Pu, X., Shu, B., Bin, S., and Lin, J. (2020). Transcriptome analysis of putative detoxification genes in the Asian citrus psyllid, *Diaphorina citri*. *Pest Manag. Sci.* 76, 3857–3870. doi:10.1002/ps.5937
- Yi, J., Wang, S., Wang, Z., Wang, X., Li, G., Zhang, X., et al. (2021). Identification of candidate carboxylesterases associated with odorant degradation in *Holotrichia parallela* antennae based on transcriptome analysis. *Front. Physiol.* 12, 674023. doi:10.3389/fphys.2021.674023
- Younus, F., Chertemps, T., Pearce, S. L., Pandey, G., Bozzolan, F., Coppin, C. W., et al. (2014). Identification of candidate odorant degrading gene/enzyme systems in the antennal transcriptome of *Drosophila melanogaster*. *Insect biochem. Mol. Biol.* 53, 30–43. doi:10.1016/j.ibmb.2014.07.003
- Yu, X., and Killiny, N. (2018). Effect of parental RNA interference of a transformer-2 homologue on female reproduction and offspring sex determination in Asian citrus psyllid. *Physiol. Entomol.* 43, 42–50. doi:10.1111/phen.12223
- Yu, X., and Killiny, N. (2020). RNA interference-mediated control of Asian citrus psyllid, the vector of the huanglongbing bacterial pathogen. *Trop. Plant Pathol.* 45, 298–305. doi:10.1007/s40858-020-00356-7
- Yu, X. D., Liu, Z. C., Huang, S. L., Chen, Z. Q., Sun, Y. W., Duan, P. F., et al. (2016). RNAi-mediated plant protection against aphids. *Pest Manag. Sci.* 72, 1090–1098. doi:10.1002/ps.4258
- Yu, X., Marshall, H., Liu, Y., Xiong, Y., Zeng, X., Yu, H., et al. (2022). Sex-specific transcription and DNA methylation landscapes of the Asian citrus psyllid, a vector of huanglongbing pathogens. *bioRxiv [Preprint]*. doi:10.1101/2022.01.28.478167
- Zhang, H., Chen, J. L., Lin, J. H., Lin, J. T., and Wu, Z. Z. (2020). Odorant-binding proteins and chemosensory proteins potentially involved in host plant recognition in the Asian citrus psyllid, *Diaphorina citri*. *Pest Manag. Sci.* 76, 2609–2618. doi:10.1002/ps.5799
- Zhou, S., and Jander, G. (2022). Molecular ecology of plant volatiles in interactions with insect herbivores. *J. Exp. Bot.* 73, 449–462. doi:10.1093/jxb/erab413
- Zhou, J. J., Vieira, F. G., He, X. L., Smadja, C., Liu, R., Rozas, J., et al. (2010). Genome annotation and comparative analyses of the odorant-binding proteins and chemosensory proteins in the pea aphid *Acyrtosiphon pisum*. *Insect Mol. Biol.* 19, 113–122. doi:10.1111/j.1365-2583.2009.00919.x
- Zhou, S. S., Sun, Z., Ma, W., Chen, W., and Wang, M. Q. (2014). *De novo* analysis of the *Nilaparvata lugens* (Stål) antenna transcriptome and expression patterns of olfactory genes. *Comp. Biochem. Physiol. Part D. Genomics Proteomics* 9, 31–39. doi:10.1016/j.cbd.2013.12.002
- Zhou, C. (2020). The status of citrus Huanglongbing in China. *Trop. Plant Pathol.* 45, 279–284. doi:10.1007/s40858-020-00363-8